Original citation:
Connaughton, Colm, Dutta, Arghya, Rajesh, R., Siddharth, Nana and Zaboronski, Oleg V. (2018) Stationary mass distribution and non-locality in models of coalescence and shattering. Physical Review E, 97 (2). 022137.

Permanent WRAP URL:
http://wrap.warwick.ac.uk/98702

Publisher statement:
© 2018 American Physical Society

Published version: https://doi.org/10.1103/PhysRevE.97.022137

Stationary mass distribution and non-locality in models of coalescence and shattering

Colm Connaughton,[1, 2, 3, *] Arghya Dutta,[4, †] R. Rajesh,[5, 6, ‡] Nana Siddharth,[5, 6, §] and Oleg Zaboronski[1, ¶]

[1] *Mathematics Institute, University of Warwick, Gibbet Hill Road, Coventry CV4 7AL, UK*
[2] *Centre for Complexity Science, University of Warwick, Coventry CV4 7AL, UK*
[3] *London Mathematical Laboratory, 14 Buckingham St. London WC2N 6DF, UK*
[4] *Université de Strasbourg, CNRS, Institut Charles Sadron, UPR 22, 67000 Strasbourg, France*
[5] *The Institute of Mathematical Sciences, CIT Campus, Taramani, Chennai 600113, India*
[6] *Homi Bhabha National Institute, Training School Complex, Anushakti Nagar, Mumbai 400094, India*
(Dated: October 6, 2017)

We study the steady state properties of models of aggregation and shattering on collision using the Smoluchowski equation. The asymptotic properties of the steady state mass distribution for a general kernel are obtained analytically by analyzing both the equations satisfied by the moments as well as the singular behavior of different generating functions. It is shown that the exponents characterizing the large and small mass asymptotic behavior of the mass distribution depends on whether the kernel is local or non-local. The non-local regime is further divided into two sub-regimes where the functional dependence of the exponents on the kernel is different. The mass distribution is shown to have logarithmic corrections at the boundaries between locality and the different regimes of non-locality. Exact solutions of special cases and numerical analysis are consistent with the general solution justifying the underlying assumptions.

I. INTRODUCTION

There is a large number of physical phenomena in which the underlying physical mechanism is coalescence when two constituents collide. Examples include hydrogels for biomedical applications [1], supramolecular polymer gels [2], aerosol formation [3], cloud formation [4, 5], ductile fracture [6], charged biopolymers [7, 8], etc. More applications and known results may be found in recent reviews [9, 10]. In a collision, it is also possible that the colliding particles may fragment or shatter into smaller particles. Whether the collision between particles will result in coagulation or fragmentation of the constituent particles depends on the energy of the colliding particles [11, 12]. Typically particles with higher kinetic energy fragment, while slow moving ones coalesce or rebound. The size distribution of the fragmented particles is typically a power law distribution [13–16], reproducible in simple tractable models [17, 18]. Such fragmentation processes find application in geophysics [19], astrophysics [20, 21], glacier modeling [22], etc.

When the two processes occur together, one might expect the system to reach a nonequilibrium steady state in which the depletion of smaller particles to create larger ones by coagulation is balanced by the depletion of larger particles to create smaller ones by fragmentation. A combination of aggregation and fragmentation is believed to be relevant to the formation and stability of planetary rings [23, 24]. In particular, simple models of binary collisions [12, 25] have been studied to explain the particle size distribution of the material constituting Saturn's rings [26]. The underlying microscopic dynamics is encoded in the collision kernel $K(i, j)$, the rate at which particles of masses i and j collide. The simplest model of fragmentation is one in which all fragmented particles are of the size of the smallest possible particle [12, 25]. We refer to such extreme fragmentation as shattering. Aggregation-shattering processes have been proposed to explain a diverse set of phenomena in addition to the application to planetary rings making a parametric study worthwhile. Examples include the statistical properties of insurgent conflicts [27], the fluctuations of phase coherent domains in high-temperature superconductors [28] and the dynamics of herding behavior in financial markets [29].

For the application to planetary rings, the relevant kernel is the one for ballistic motion in three dimensions. This corresponds to $K(i, j) \propto |m_1^{-1/2} - m_2^{-1/2}|(m_1^{1/3} + m_2^{1/3})^2$, where the first factor accounts for relative velocity and the second to the area of cross section. However, the asymptotic behavior of the steady state mass distribution is believed to possess universality with respect to details of the kernel and expected to depend on only two exponents characterizing the kernel. A generic homogeneous collision kernel that captures the essence of many more complicated collision kernels is $K(i, j) = i^\mu j^\nu + i^\nu j^\mu$, characterized by exponents μ, ν or equivalently by homogeneity exponent $\beta = \mu + \nu$ and locality exponent $\theta = \nu - \mu$ (see Refs. [9, 10] for kernels for different physical phenomena). In this paper, locality refers to the dynamics in mass space. The aggregation kinetics are said to be local if particles typically grow by merging with particles of comparable size and nonlo-

* C.P.Connaughton@warwick.ac.uk
† argphy@gmail.com
‡ rrajesh@imsc.res.in
§ nana.siddharth@gmail.com
¶ olegz@maths.warwick.ac.uk

cal if particles typically grow by merging with particles that are much larger or much smaller than themselves. Whether the steady state kinetics are local or nonlocal depends on the value of θ [30]. In terms of scaling, the ballistic kernel corresponds to $\beta = 1/6$ and $\theta = 7/6$. For the above generic kernel with these exponents, it was not possible to solve for the mass distribution even within the mean field approximation corresponding to Smoluchowski equation. As a further approximation, it was assumed that the mass distribution is universal with respect to θ, and therefore may be obtained by solving for the kernel $K(i,j) = (ij)^{1/12}$ within the Smoluchowski equation [31]. The resulting mass distribution is in excellent agreement with observed size distribution of the rings of Saturn [12, 25].

In a recent paper, we studied the steady state mass distribution of a related non-conserved system with coalescence, input of small particles and collision-dependent evaporation [32]. The difference from the conserved model, where total mass is strictly a constant, is that on collision, particles do not fragment, but are removed from system, and hence mass is no longer conserved. For this model it was possible to determine the asymptotic behavior of the mass distribution for kernels with arbitrary β and θ. In particular, we showed that the mass distribution is sensitive to the locality exponent θ. The results for $\theta > 1$ are different from that for $\theta < 1$, and the mass distributions for $\theta > 1$ are nonuniversal in the sense that they depend on the driving and dissipation scales. Given that $\theta > 1$ for the ballistic kernel, it stands to reason that the assumption of the mass distribution being independent of θ in the conserved model [12, 25] may result in erroneous results.

Do the results for the conserved model with collision dependent fragmentation depend on the locality exponent θ? In this paper, we do a detailed analysis of the conserved model for arbitrary β and θ. The asymptotic behavior of the mass distribution is determined using scaling, moment analysis, and singularity analysis, all of which are confirmed through a numerical solution. In particular, we show that the results are dependent on the locality exponent θ. There is a local regime ($\theta < 1$) and two nonlocal regimes: $1 < \theta < 2$ and $2 < \theta$. When the dependence on θ is taken onto account correctly, with respect to the ballistic kernel, we show that radius distribution of particles is $r^{-5/2}$ instead of $r^{-11/4}$ obtained in Ref. [12, 25], where r is the radius of the particle.

The remainder of the paper is organized as follows. In Sec. II we define the model precisely and state our main results. In Sec. III we discuss the numerical algorithm that we use to solve for the steady state mass distribution. It is an iterative procedure that that we show to reproduce known exact solutions. In Sec. IV we solve the model exactly for 2 special cases: first when $\mu = \nu$ and second the addition model in which two particles coalesce only when at least one particle is a monomer. These exact solutions help us to benchmark the numerical algorithm. It is possible to obtain exact results for integer θ. This is discussed in Sec. V, where the presence of logarithmic corrections is established for some values of θ. In Sec. VI, the small mass behavior of the mass distribution is studied using the exact relations between different moments. This enables us to determine the exponents when the kernel is local, and relations between the exponents when the kernel is non-local. In Sec. VII, we analyze the large mass behavior of the mass distribution by studying the singularities of the generating functions. By stitching together the small and large mass behavior, we are able to determine both the small and large mass asymptotic behavior of the mass distribution. Finally we conclude with a overview of results and directions of future research in Sec. VIII.

II. MODEL

Consider a collection of particles, each characterized by a single scalar parameter, mass. The mass of particle i will be denoted by m_i, $i = 1, 2, \ldots$, and will be measured in terms of the smallest possible mass in the system m_0, corresponding to the smallest possible dust particle, such that m_i is an integer. Given a certain initial configuration, the system evolves in time via coagulation and collision-dependent fragmentation. Two particles of masses m_1 and m_2 collide at rate $(1 + \lambda)K(m_1, m_2)$, where $K(m_1, m_2)$ is the collision kernel. On collision, with probability $1/(1 + \lambda)$, the two particles coalesce to form a particle of mass $m_1 + m_2$, and with probability $\lambda/(1 + \lambda)$, fragment into $(m_1 + m_2)$ particles of mass 1. Note that both the dynamical processes conserve mass, so that total mass is a constant of motion. We would be interested in the limiting case when the fragmentation rate tends to zero, ie, $\lambda \to 0$. Also, we will be considering the well-mixed mean field limit when the spatial correlations between the particles may be neglected.

Let $N(m, t)$ denote the number of particles or mass m per unit volume at time t. In the well-mixed dilute limit, the time evolution of $N(m, t)$ is described by the Smoluchowski equation:

$$\frac{dN(m,t)}{dt} = \frac{1}{2} \sum_{m_1=1}^{\infty} \sum_{m_2=1}^{\infty} N(m_1,t)N(m_2,t)K(m_1,m_2)\delta(m_1+m_2-m) - (1+\lambda) \sum_{m_1=1}^{\infty} N(m_1,t)N(m,t)K(m_1,m)$$
$$+ \frac{\lambda}{2}\delta_{m,1} \sum_{m_1=1}^{\infty} \sum_{m_2=1}^{\infty} N(m_1,t)N(m_2,t)K(m_1,m_2)(m_1+m_2). \tag{1}$$

The first term in the right hand side of Eq. (1) is a gain term that accounts for the number of ways a particle of mass m may be created through a coalescence event. The second term is a loss term that accounts for the number of ways in which $N(m,t)$ decreases due to coalescence or fragmentation. The last term describes the creation of

particles of mass 1 due to fragmentation events. It is easy to check that the the mean mass density is conserved. In this paper, we will be interested in the steady state solution of Eq. (1) obtained by setting the time derivative to 0. We will denote the steady state solution by $N(m)$. $N(m)$ satisfies the equation

$$0 = \frac{1}{2} \sum_{m_1=1}^{\infty} \sum_{m_2=1}^{\infty} N(m_1,t)N(m_2,t)K(m_1,m_2)\delta(m_1+m_2-m) - (1+\lambda) \sum_{m_1=1}^{\infty} N(m_1,t)N(m,t)K(m_1,m)$$
$$+ \frac{\lambda}{2}\delta_{m,1} \sum_{m_1=1}^{\infty} \sum_{m_2=1}^{\infty} N(m_1,t)N(m_2,t)K(m_1,m_2)(m_1+m_2). \tag{2}$$

We consider the general class of kernels given by

$$K(m_1,m_2) = m_1^\mu m_2^\nu + m_1^\nu m_2^\mu, \quad \nu \geq \mu. \tag{3}$$

The kernel may also be classified using two other exponents. The first is the homogeneity exponent β defined through $K(hm_1,hm_2) = h^\beta K(m_1,m_2)$:

$$\beta = \nu + \mu. \tag{4}$$

Second is the nonlocality exponent θ defined as

$$\theta = \nu - \mu. \tag{5}$$

When $\beta > 1$, the kernel is referred to as a gelling kernel and non-gelling otherwise. We will refer to kernels with $\theta < 1$ as local kernels and non-local otherwise.

We also consider another kernel that corresponds to the so called addition model [33–38] . Here collision events are allowed only if at least one of the particles has mass 1. The kernel for the addition model is

$$K^{add}(m_1,m_2) = m_1^\nu m_2^\nu(\delta_{m_1,1} + \delta_{m_2,1}), \tag{6}$$

which is characterized by a single exponent ν. This kernel turns out to be exactly solvable (see Sec. IV B).

In this paper, we will determine the asymptotic behavior of $N(m)$ through analysis of the moments as well as the singularities. Moments and generating function are

TABLE I. Summary of results obtained in this paper. The exponents y, τ_s, η_s, τ_ℓ, and η_ℓ are as defined in Eqs. (11), (12), and (13). For $\theta = 1$ and $\theta = 2$, there are additional logarithmic corrections as described in Eqs. (78) and (57) respectively.

θ	y	τ_s	η_s	τ_ℓ	η_ℓ
0	2	$\frac{3+\beta}{2}$	$\min[0, \frac{1-\beta}{2}]$	$\frac{3+\beta}{2}$	$\min[0, \frac{1-\beta}{2}]$
$(0,1)$	$\frac{2}{\theta+1}$	$\frac{3+\beta}{2}$	$\max[\frac{1-\beta}{2}, 0]$	$\frac{2+\beta}{2}$	$\max[\frac{2-\beta}{2}, \frac{1}{2}]$
$(1,2)$	1	$\mu+2$	$\max[-\mu, 0]$	$\frac{2+\beta}{2}$	$\eta_s + \frac{2-\theta}{2}$
$(2,\infty)$	1	ν	$\max[2-\nu, 0]$	ν	$\max[2-\nu, 0]$

defined as:

$$\mathcal{M}_\alpha = \sum_{m=1}^{\infty} m^\alpha N(m), \tag{7}$$

$$F_\alpha(x) = \sum_{m=1}^{\infty} m^\alpha N(m)x^m. \tag{8}$$

Clearly $F_\alpha(1) = \mathcal{M}_\alpha$. Multiplying Eq. (2) by x^m and summing over all m, we obtain a relation between moments and generating functions,

$$F_\mu(x)F_\nu(x) - (1+\lambda)\left[\mathcal{M}_\mu F_\nu(x) + \mathcal{M}_\nu F_\mu(x)\right]$$
$$+ x(1+2\lambda)\mathcal{M}_\mu \mathcal{M}_\nu = 0. \tag{9}$$

We also define the exponents that characterize the mass distribution $N(m)$. We assume that the only rele-

vant mass scale in the problem is the cutoff mass M and hence $N(m)$ has the scaling form:

$$N(m) = m^{-\tau} f\left(\frac{m}{M}\right), \quad m, M \gg 1, \qquad (10)$$

where τ is an exponent and $f(x)$ is a scaling function. M denotes the cutoff scale below and above which $N(m)$ behaves differently. There are two cutoff mass scales in the problem. One is the total mass in the system and the other is the scale introduced by fragmentation. We will be working in the limit when total mass is infinite, but mean density is finite, leaving only one cutoff scale. The divergence of the cutoff mass scale as the fragmentation rate $\lambda \to 0$ is captured by

$$M \sim \lambda^{-y}, \quad \lambda \to 0, \qquad (11)$$

where the exponent y will depend on the kernel. To characterize the scaling behavior for small and large masses, we introduce four new exponents τ_s, η_s, τ_ℓ and η_ℓ which are defined as:

$$N(m) \simeq \frac{a_s}{m^{\tau_s} M^{\eta_s}}, \quad m \ll M, \qquad (12)$$

$$N(m) \simeq \frac{a_\ell}{m^{\tau_\ell} M^{\eta_\ell}} e^{-m/M}, \quad m \gg M. \qquad (13)$$

The exponential decay for large mass is a conjecture. For $m \gg M$, the exponential decay with mass will be supported by exact solutions for special cases and numerical observation for more general cases. Further justification for arbitrary kernels follows from the additivity principle using which it has been argued that, for generic conserved mass models, the mass distribution has an exponential decay [39, 40]. The four exponents are not independent. It is straightforward to obtain from Eq. (10) that

$$\tau_s + \eta_s = \tau_\ell + \eta_\ell = \tau. \qquad (14)$$

The results obtained in this paper for the different exponent as a function of the exponents θ and β are summarized in Table. I.

III.   NUMERICAL ALGORITHM

In this section, we describe the numerical scheme for obtaining the steady state mass distribution $N(m)$. Solving Eq. (2) in the steady state for $m = 1$, we obtain

$$N(1) = \frac{2\lambda + 1}{1 + \lambda} \frac{\mathcal{M}_\mu \mathcal{M}_\nu}{\mathcal{M}_\mu + \mathcal{M}_\nu}. \qquad (15)$$

For $m \geq 2$, $N(m)$ may be determined from Eq. (2) in the steady state, provided $\mathcal{M}_\mu$, $\mathcal{M}_\nu$, and all $N(k)$ for $k < m$ are known:

$$N(m) = \frac{\displaystyle\sum_{m_1=1}^{m-1} N(m_1)N(m-m_1)K(m_1, m-m_1)}{2(1+\lambda)(m^\mu \mathcal{M}_\nu + m^\nu \mathcal{M}_\mu)}. \qquad (16)$$
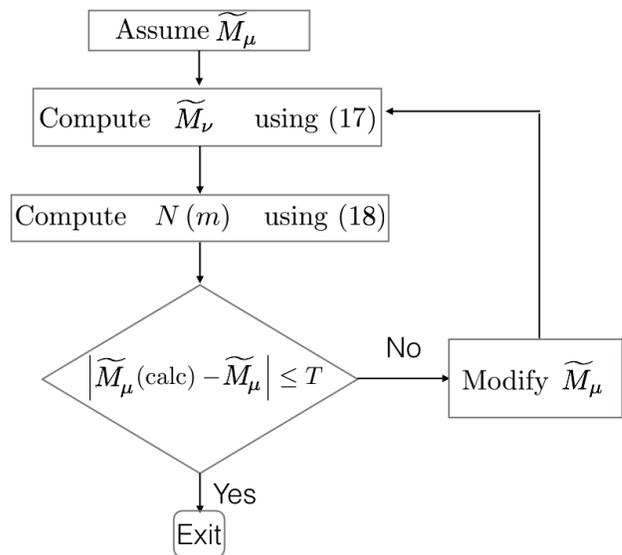

FIG. 1. Flowchart describing the iterative numerical algorithm for determining the steady state distribution $N(m)$.

Thus, $\mathcal{M}_\mu$ and $\mathcal{M}_\nu$ determine $N(m)$ for $m \geq 1$.

Consider scaled variables $\widetilde{N}_m = N(m)/N(1)$ and $\widetilde{\mathcal{M}}_\alpha = \mathcal{M}_\alpha/N(1)$. In terms of these variables, Eq. (15) and Eq. (16) reduce to

$$1 = \frac{2\lambda + 1}{1 + \lambda} \frac{\widetilde{\mathcal{M}}_\mu \widetilde{\mathcal{M}}_\nu}{\widetilde{\mathcal{M}}_\mu + \widetilde{\mathcal{M}}_\nu}, \qquad (17)$$

$$\widetilde{N}(m) = \frac{\displaystyle\sum_{m_1=1}^{m-1} \widetilde{N}(m_1)\widetilde{N}(m-m_1)K(m_1, m-m_1)}{2(1+\lambda)(m^\mu \widetilde{\mathcal{M}}_\nu + m^\nu \widetilde{\mathcal{M}}_\mu)} \qquad (18)$$

$\widetilde{\mathcal{M}}_\mu$ and $\widetilde{\mathcal{M}}_\nu$ determine $\widetilde{N}(m)$ for $m \geq 1$. The two unknowns, $\widetilde{\mathcal{M}}_\mu$ and $\widetilde{\mathcal{M}}_\nu$ are not independent and related to each other through Eq. (17).

To determine $\widetilde{\mathcal{M}}_\mu$, we follow an iterative procedure as summarized in the flowchart shown in Fig. 1. We start by assigning a numerical value (close to 1.0) for $\widetilde{\mathcal{M}}_\mu$. $\widetilde{\mathcal{M}}_\nu$ is determined from Eq. (17). We then solve for $\widetilde{N}(m)$ up to a value of m for which $\widetilde{N}(m)$ is larger than a predetermined value (10^{-16} in our analysis), setting $N(m) = 0$ for larger values of m. We then check for self consistency, i.e whether $\sum m^\mu \widetilde{N}(m)$ is equal to the preassigned value of $\widetilde{\mathcal{M}}_\mu$. We increment $\widetilde{\mathcal{M}}_\mu$ in small steps till the self consistency condition is satisfied to the required precision. In our numerical analysis, we demand that the difference between the assumed and calculated values of $\widetilde{\mathcal{M}}_\mu$ should be smaller than 10^{-10}.

To determine the unscaled variables $N(m)$, we use the fact that mass is conserved: $\sum_1^\infty mN(m) = \rho$, where ρ will be treated as a parameter. We then scale all $\widetilde{N}(m)$ by the same factor so that the desired mass density ρ is

achieved, thereby determining $N(m)$. In our numerical measurements, we set $\rho = 1$. There is no proof that the algorithm will result in the convergence of $N(m)$ to its correct value. However, we verify the convergence for special solvable kernels (see Sec. IV), leading us to expect that the mass distribution converges to its correct value for more general kernels.

From the numerically computed $N(m)$, we observe that, for all values of μ and ν that we have studied, $N(m)$ decays exponentially at large masses [as in Eq. (13)]. The exponential cutoff mass M is determined by solving for the three parameters (τ_ℓ, M, and a_ℓ/M^{η_ℓ}) in Eq. (13) using $N(m)$ for three consecutive m's and extrapolating to large m. Once M is determined, the compensated mass distribution $N(m)e^{m/M}$ is a power law with exponent τ_ℓ, allowing us to verify the theoretical results for the exponents at large mass.

IV. EXACT SOLUTIONS

The steady state mass distribution $N(m)$ may be determined exactly for two cases: 1) when $\mu = \nu = \beta/2$ and 2) the addition model (defined in Sec. IV B).

A. $\mu = \nu = \beta/2$ ($\theta = 0$)

When $\mu = \nu = \beta/2$, the kernel Eq. (3) reduces to the multiplicative kernel. In this case, Eq. (9) for the generating function reduces to the quadratic equation

$$F_{\beta/2}^2(x) - 2(1+\lambda)\mathcal{M}_{\beta/2}F_{\beta/2}(x) + x(1+2\lambda)\mathcal{M}_{\beta/2}^2 = 0 \tag{19}$$

which may be solved to yield

$$F_{\beta/2}(x) = (1+\lambda)\mathcal{M}_{\beta/2}\left[1 - \sqrt{1 - \frac{x}{x_c}}\right], \tag{20}$$

where

$$x_c = \frac{(1+\lambda)^2}{(1+2\lambda)}, \tag{21}$$

and the sign of the square-root of the discriminant is fixed by the constraint $F_\mu(0) = 0$. The coefficient of x^m is the Taylor expansion of $F_\mu(x)$ is $N(m)$ and is:

$$N(m) = \frac{(2m-2)!}{2^{2m-1}m!(m-1)!}\frac{\mathcal{M}_{\beta/2}(1+\lambda)}{m^{\beta/2}x_c^m}, \ m = 1, 2, \ldots \tag{22}$$

For large m, the factorials may be approximated using Stirling formula, and the asymptotic behavior of $N(m)$ for large m may be derived to be

$$N(m) \simeq \frac{\mathcal{M}_{\beta/2}(1+\lambda)}{2\sqrt{\pi}}\frac{e^{-m/M}}{m^{(3+\beta)/2}}, \ m \gg 1, \tag{23}$$

where

$$M = \frac{1}{\lambda^2}, \ \lambda \to 0, \tag{24}$$

or equivalently the exponent $y = 2$.

In Eq. (23), $\mathcal{M}_{\beta/2}$ is determined by the condition that $\mathcal{M}_1 = \rho$ is a constant. It is not possible to find a closed form expression for $\mathcal{M}_{\beta/2}$ for arbitrary β, however when $\beta/2$ is an integer, it is possible to compute by differentiating or integrating Eq. (20) with respect to x and setting $x = 1$. It is then straightforward to obtain $\mathcal{M}_0 = \frac{2\lambda}{1+2\lambda}\rho$ for $\beta = 0$, and $\mathcal{M}_1 = \rho$ for $\beta = 2$. For generic β, we use the asymptotic form Eq. (23) to obtain the dependence of $\langle m \rangle$ on the cutoff, thus determining $\mathcal{M}_{\beta/2}$. We thus obtain

$$N(m) \propto \frac{\rho}{M^{\min[0,(1-\beta)/2]}}\frac{e^{-m\lambda^2}}{m^{(3+\beta)/2}}, \quad \theta = 0. \tag{25}$$

In the limit of $\lambda \to 0$, $N(m)$ tends to a finite limit only when the kernel is gelling, ie $\beta > 1$. For non-gelling kernels with $\beta < 1$, the prefactor tends to zero with decreasing fragmentation rate λ. This observation may be rationalized by the fact the the mass capacity of gelling kernels is finite and infinite for non-gelling kernels. Summarizing the results for $\theta = 0$, we have derived the results

$$\tau_s = \tau_\ell = \frac{3+\beta}{2}, \tag{26a}$$

$$\eta_s = \eta_\ell = \min[0, (1-\beta)/2], \quad \theta = 0, \tag{26b}$$

$$y = 2. \tag{26c}$$

The exact solution for the case $\mu = \nu$ (see Sec. IV) is used to benchmark the numerical scheme. In Fig. 2, we plot the numerical solution to Eq. (2), obtained using the aforementioned algorithm, for four different values of μ. The numerically determined cutoff scale M is in excellent agreement with the exact solution (see inset of Fig. 2). The data for the compensated mass distribution $N(m)e^{m/M}$ are power laws with exponents matching the ones obtained from the exact solution (see Fig. 2). We thus conclude that the numerical scheme is accurate and stable.

B. Addition model with fragmentation

In this section, we calculate $N(m)$ for the addition model. In this case, collisions between particles are allowed only if at least one of the masses is one, and the resulting collision kernel is as in Eq. (6). While this model is expected to mimic the kernel Eq. (3) with $\nu \gg \mu$ when collisions between dissimilar masses dominate, the exact regime of applicability will become clear only on comparing with the full solution for $N(m)$. For the addition model, the Smoluchowski equation Eq. (2) in the steady
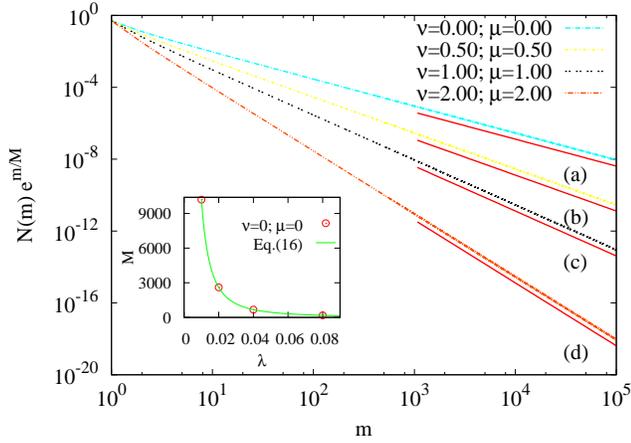
FIG. 2. $N(m)e^{m/M}$ when $\nu = \mu$ for $\nu = 0, 1/2, 1, 2$. The solid lines are power laws with an exponent $-(3 + \beta)/2$: (a) $-3/2$, (b) -2, (c) $-5/2$, and (d) $-7/2$. The evaporation rate is $\lambda = 0.01$. Inset: M, obtained from numerical analysis, is compared with the the analytical result in Eq. (21).

state is

$$
0 = N(1)\left[(m-1)^{\nu}N(m-1) - (1+\lambda)m^{\nu}N(m)\right] \\
+ \delta_{m,1}\left[\lambda N(1)(N_{\nu} + N_{\nu+1}) - (1+\lambda)N_{\nu}N(m)m^{\nu}\right]. \tag{27}
$$

This is easily solved to give

$$
N(m) = \frac{\lambda \mathcal{M}_{\nu+1} - \mathcal{M}_{\nu}}{m^{\nu}(1+\lambda)^m}, \quad m = 1, 2, \ldots, \tag{28}
$$

which in the limit of large mass and vanishing λ reduces to

$$
N(m) \simeq \frac{N(1)}{m^{\nu}}e^{-m/M}, \quad m \gg 1, \tag{29}
$$

where $M = \lambda^{-1}[1 + O(\lambda)]$. The unknown parameter $N(1)$ is determined by the constraint that mass is conserved: $\sum_1^{\infty} mN(m) = \rho$. We thus obtain

$$
N(m) \propto \frac{\rho}{M^{\max[2-\nu,0]}}\frac{e^{-m/M}}{m^{\nu}}, \quad m \gg 1. \tag{30}
$$

To summarize, we have obtained

$$
\tau_s = \tau_{\ell} = \nu, \tag{31a}
$$
$$
\eta_s = \eta_{\ell} = \max[0, 2 - \nu], \tag{31b}
$$
$$
y = 1, \tag{31c}
$$

for the addition model.

V. MASS DISTRIBUTION FOR INTEGER θ

It is possible to obtain exact results for the case when the locality exponent θ is an integer, namely $\theta = n$, n is

an integer. The starting point is Eq. (9). If $\nu = \mu + n$, where $n = 1, 2, \ldots$, Eq. (9) reduces to a closed differential equation for F_{μ}:

$$
[F_{\mu}(x) - (1+\lambda)\mathcal{M}_{\mu}](x\partial_x)^n F_{\mu}(x) - (1+\lambda)\mathcal{M}_{\nu}F_{\mu}(x) \\
+ x(1+2\lambda)\mathcal{M}_{\mu}\mathcal{M}_{\nu} = 0. \tag{32}
$$

We expect the singularities to occur at the points in the complex x-plane where the coefficient in front of the highest order term is zero. Therefore, at the singular point x_c, F_{μ} satisfies

$$
F_{\mu}(x_c) = (1+\lambda)\mathcal{M}_{\mu}. \tag{33}
$$

Introduce new variables $f(x)$ as follows:

$$
F_{\mu}(x) = (1+\lambda)\mathcal{M}_{\mu} + f(x), \tag{34}
$$
$$
t = \ln(x), \tag{35}
$$

where $f(x_c) = 0$ and $t_c = \ln(x_c) > 0$. Then Eq. (32) may be rewritten as

$$
f\partial_t^n f - (1+\lambda)\mathcal{M}_{\nu}f - (1+2\lambda)\mathcal{M}_{\mu}\mathcal{M}_{\nu}\left[\frac{(1+\lambda)^2}{(1+2\lambda)} - e^t\right] = 0. \tag{36}
$$

Equation (36) becomes more tractable under the following transformations:

$$
t = \ln\left(\frac{(1+\lambda)^2}{(1+2\lambda)}\right) + \tau, \tag{37}
$$
$$
f(t) = (1+\lambda)\mathcal{M}_{\nu}g(\tau), \tag{38}
$$

such that we obtain

$$
g(\tau)\partial_{\tau}^n g(\tau) - g(\tau) - j(1 - e^{\tau}) = 0, \tag{39}
$$

where

$$
j = \frac{\mathcal{M}_{\mu}}{\mathcal{M}_{\nu}}. \tag{40}
$$

We note that $g(\tau_c) = 0$. We now analyze Eq. (39) for specific integer values of θ.

A. $\theta = 1$

When $n = 1$, near the critical point Eq. (39) reduces to

$$
gg' = j(1 - e^{\tau_c}) + o(1), \tag{41}
$$

since $g(\tau_c) = 0$. Solving for $g(\tau)$, we obtain

$$
g(\tau) = \sqrt{2j(e^{\tau_c} - 1)}\sqrt{\tau_c - \tau} + o(\sqrt{\tau_c - \tau}). \tag{42}
$$

The generating function g must be real for $\tau \in \mathbf{R}$, $\tau < \tau_c$. Therefore we must have $\tau_c > 0$ or in terms of the original variables,

$$
x_c > \frac{(1+\lambda)^2}{(2\lambda + 1)}. \tag{43}
$$

We conclude that for $\theta = 1$,

$$f(x) = A\sqrt{x_c - x} + o(\sqrt{x_c - x}), \qquad (44)$$

where the amplitude is

$$A = \sqrt{2(1 + 2\lambda)\mathcal{M}_\mu\mathcal{M}_\nu \left[1 - \frac{(1+\lambda)^2}{(1+2\lambda)}x_c^{-1}\right]}. \qquad (45)$$

We conclude that in the limit of large masses,

$$N_\mu(m) \sim A \int_0^\infty \frac{dx}{\pi}(x_c + x)^{-m-1}\sqrt{x} \qquad (46)$$

$$\sim \frac{Ax_c^{1/2}}{2\sqrt{\pi}}m^{-3/2}e^{-m\ln(x_c)}. \qquad (47)$$

Equivalently,

$$N(m) \sim \sqrt{\frac{(1+2\lambda)\mathcal{M}_\mu\mathcal{M}_\nu}{2\pi}\left[x_c - \frac{(1+\lambda)^2}{(1+2\lambda)}\right]}\frac{x_c^{-m}}{m^{\mu+3/2}}. \qquad (48)$$

An independent moment equations analysis shows that for $\lambda \downarrow 0$ [see Eqs. (75a) and (83)],

$$x_c = 1 + \frac{1}{M}, \quad \text{where } M \sim \lambda^{-1}. \qquad (49)$$

Then the small λ limit of Eq. (48) is

$$N(m) \sim \sqrt{\frac{\mathcal{M}_\mu\mathcal{M}_\nu}{2\pi M}}\frac{e^{-m/M}}{m^{(2+\beta)/2}}, \quad \theta = 1. \qquad (50)$$

B. $\theta = 2$

When $n = 2$, near the critical point Eq. (39) reduces to

$$gg'' = j(1 - e^{\tau_c}) + o(1), \quad g(\tau_c) = 0, \qquad (51)$$

which has a solution given by

$$g(\tau) = \sqrt{2j(e^{\tau_c} - 1)\ln\frac{\Delta}{\tau_c - \tau}}(\tau_c - \tau) + \dots,$$

where Δ is a positive constant which sets a reference scale in τ-space. Notice that the solution depends on an arbitrary constant Δ, which is consistent with the solution of a second order ordinary differential equation subject to a single boundary condition $g(\tau_c) = 0$. In principle, Δ may be determined by matching this singularity dominated solution with the solution far from the singular point. In the original variables this reads as

$$f(y) = \sqrt{2J\left[x_c - \frac{(1+\lambda)^2}{(1+2\lambda)}\right]\frac{y}{x_c}\sqrt{\ln\frac{\Delta x_c}{y}}} + \dots, (52)$$

where $y = x_c - x$, and

$$J = (1 + 2\lambda)\mathcal{M}_\mu\mathcal{M}_\nu. \qquad (53)$$

Calculating the jump over the branch cut singularity of f, we find that

$$N_\mu(m) = \sqrt{\frac{J}{2}\left[x_c - \frac{(1+\lambda)^2}{1+2\lambda}\right]}\int_0^\infty dy \frac{y[\ln\frac{\Delta x_c}{y}]^{-1/2}}{x_c(x_c + y)^{m+1}} + \dots \qquad (54)$$

Changing variables $y \to yx_c/m$ and taking the large-m limit of the integral we obtain

$$N(m) \sim \sqrt{\frac{J}{2}\left[x_c - \frac{(1+\lambda)^2}{(1+2\lambda)}\right]}\frac{e^{-m\ln x_c}}{m^\nu\sqrt{\ln\frac{m}{m_0}}}, \qquad (55)$$

where m_0 is a reference scale in the mass space.

In the limit of small λ, we expect that [see Eqs. (75a) and (83)]

$$x_c = 1 + \frac{1}{M}, \quad \text{where } M \sim \lambda^{-1}. \qquad (56)$$

Then Eq. (55) simplifies to

$$N(m) \sim \sqrt{\frac{\mathcal{M}_\mu\mathcal{M}_\nu}{2M}}\frac{e^{-m/M}}{m^\nu\sqrt{\ln\frac{m}{m_0}}}, \qquad (57)$$

Therefore, we find that that there are logarithmic corrections to the scaling form, and $\theta = 2$, $\tau_\ell = \nu$, $\eta_\ell = 1/2$ and $a_\ell = \sqrt{J/2}$.

C. $\theta = 3, 4, \dots$

Finally, we analyze Eq. (39) for $n > 2$. Near the critical point,

$$g(\tau)\partial_\tau^n g(\tau) = j(1 - e^{\tau_c}) + \dots. \qquad (58)$$

We try the family of solutions:

$$g(\tau) = p_{n-2}(\tau_c - \tau) + A(\tau_c - \tau)^{n-1}\log\left(\frac{\Delta}{\tau_c - \tau}\right) + \dots, \qquad (59)$$

where p_{n-2} is a polynomial of $(n-1)$-st degree such that $p_{n-2}(0) = 0$,

$$p_n(x) = d_1 x + d_2 x^2 + \dots + d_{n-2}x^{n-2}. \qquad (60)$$

Note that Eq. (59) depends on n arbitrary constants (before we impose the condition $g(\tau_c) = 0$), which makes it a good candidate for a general solution. Differentiating the above Ansatz, we find:

$$\partial_\tau^n g(\tau) = (-1)^n n!\frac{A}{\tau_c - \tau} \qquad (61)$$

Substituting this into Eq. (58) gives an answer for the amplitude:

$$A = \frac{(-1)^{n-1}}{(n-1)!} \cdot \frac{j(1 - e^{\tau_c})}{d_1}. \qquad (62)$$

The coefficient d_1 can be expressed in terms of $F_{\mu+1}$: it follows from the definition of F_μ that

$$d_1 = \partial_\tau g(x_c) = \frac{F_{\mu+1}(x_c)}{(1+\lambda)\mathcal{M}_\nu} \tag{63}$$

Applying the inversion formula and using the fact that the analytic part of $g(\tau)$ does not contribute to the large mass asymptotic, one finds that

$$N(m) \sim \frac{J}{F_{\mu+1}(x_c)}\left[x_c - \frac{(1+\lambda)^2}{1+2\lambda}\right]\frac{e^{-m\ln(x_c)}}{m^\nu}. \tag{64}$$

For small λ's,

$$N(m) \sim \frac{\mathcal{M}_\mu \mathcal{M}_\nu}{MF_{\mu+1}(x_c)}\frac{e^{-m/M}}{m^\nu}, \; m \gg M, \; \theta = 3,4,\ldots \tag{65}$$

The logarithmic corrections to the mass distribution for integer θ, calculated in this section may be summarized as follows:

$$N(m) \approx \frac{a_\ell e^{-m/M}}{m^\nu(\ln m)^\alpha}, \; m \gg M, \; \theta = 2,3,\ldots, \tag{66}$$

where $\alpha = 1/2$ for $\theta = 2$ and zero otherwise. We also note that these results coincide with the results obtained using analysis of singularities for non-integer $\theta > 2$ [see Eq. (104)]. The solution Eq. (66) is now verified using the numerical solution for N(m) for integer θ. Equation (66) has three unknown parameters a_ℓ, M and α. These parameters are determined as a function of m by using $N(m)$ for three consecutive m. The variation of α with m is shown in Fig. 3. In these data, a large value of λ ($\lambda = 20.0$) is chosen so that the small mass regime is suppressed and the large mass regime is exaggerated. It can be seen from Fig. 3 that the exponents converge, albeit slowly, to their predicted theoretical values [see Eq. (66)].

VI. MOMENT ANALYSIS

An exact solution is possible only when $\theta = 0$. In this section, we use moment analysis to determine some of the exponents characterizing $N(m)$ for general θ and β. In particular, we study the small mass behavior of the mass distribution $N(m)$ as described by Eq. (12). Our aim is to determine the exponents τ_s, η_s, and y as a function of β and θ. For this, we will require the equations satisfied by the different moments of m. These may be obtained by differentiating Eq. (9) with respect to x or by multiplying Eq. (2) by m^n and summing over m from 1 to ∞. Doing so gives

$$\lambda(\mathcal{M}_{\mu+n}\mathcal{M}_\nu + \mathcal{M}_\mu\mathcal{M}_{\nu+n}) = (1+2\lambda)\mathcal{M}_\mu\mathcal{M}_\nu$$

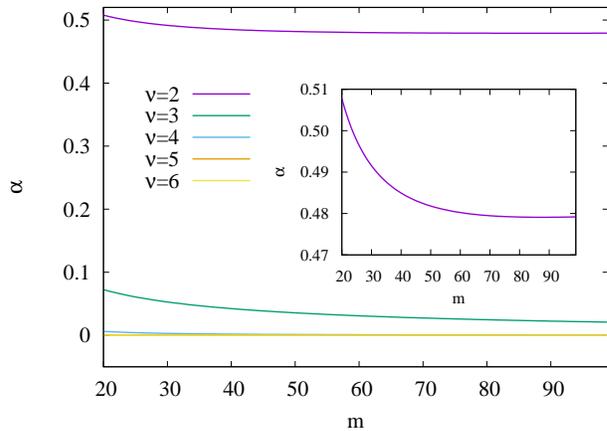$$+(1-\delta_{n,0})\sum_{r=1}^{n-1}\binom{n}{r}\mathcal{M}_{\mu+r}\mathcal{M}_{\nu+n-r}, \; n = 0,1,\ldots \tag{67}$$

FIG. 3. Variation of the exponent α characterizing the logarithmic corrections [see Eq. (66)] with m for different values of ν. The data are for $\mu = 0$, $\lambda = 20.0$, and different ν. The exponent α converges to $\alpha = 0$ ($\nu \neq 2$), and $\alpha = 1/2$ ($\nu = 2$). Inset: The variation α with m for $\nu = 2$ is shown separately for clarity.

which for $n = 0, 2$ may be explicitly written as

$$\lambda(\mathcal{M}_{\mu+1}\mathcal{M}_\nu + \mathcal{M}_\mu\mathcal{M}_{\nu+1}) = (1+2\lambda)\mathcal{M}_\mu\mathcal{M}_\nu, \tag{68a}$$

$$\lambda(\mathcal{M}_{\mu+2}\mathcal{M}_\nu + \mathcal{M}_\mu\mathcal{M}_{\nu+2}) = 2\mathcal{M}_{\mu+1}\mathcal{M}_{\nu+1}$$
$$+ (1+2\lambda)\mathcal{M}_\mu\mathcal{M}_\nu. \tag{68b}$$

Given the small mass behavior of $N(m)$ as in Eq. (12), the dependence of the α-th moment of mass on the cutoff mass M may be determined as:

$$\mathcal{M}_\alpha \sim a_s M^{-\eta_s}\int^M dm \; m^{\alpha-\tau_s}, \tag{69}$$

where by $x \sim y$, we mean that $x/y = O(M^0)$ when $\lambda \to 0$. There is no divergence at small masses as the integral is cut off at the smallest mass $m_0 = 1$. Thus, we obtain

$$\mathcal{M}_\alpha \sim \begin{cases} M^{-\eta_s}\ln M, & \alpha = \tau_s - 1, \\ M^{-\eta_s+\max(\alpha+1-\tau_s,0)}, & \alpha \neq \tau_s - 1. \end{cases} \tag{70}$$

We first derive upper and lower bounds for the exponent τ_s. We first show that $\tau_s < \nu + 2$. Assume that $\tau_s > \nu + 2$. We immediately obtain from Eq. (70) that $\mathcal{M}_\mu \sim \mathcal{M}_{\mu+1} \sim \mathcal{M}_\nu \sim \mathcal{M}_{\nu+1} \sim M^{-\eta_s}$. In this case, Eq. (68a) simplifies to $\lambda M^{-2\eta_s} \sim M^{-2\eta_s}$ or equivalently $\lambda \sim O(1)$. But λ is a parameter which tends to 0, hence we arrive at a contradiction. Hence, $\tau_s \leq \nu + 2$. We now show that $\tau_s \neq \nu+2$. Assume $\tau_s = \nu+2$. We immediately obtain from Eq. (70) that $\mathcal{M}_\mu \sim \mathcal{M}_{\mu+1} \sim \mathcal{M}_\nu \sim M^{-\eta_s}$, and $\mathcal{M}_{\nu+1} \sim M^{-\eta_s}\ln M$. It is then straightforward to obtain from Eq. (68a) that $\lambda \sim 1/\ln M$. Knowing that $\mathcal{M}_{\nu+2} \sim M^{1-\eta_s}$, Eq. (68b) simplifies to $\lambda M \sim \ln M$ or $\lambda \sim M^{-1}\ln M$, in contradiction with the earlier result $\lambda \sim 1/\ln M$. Hence, we conclude that $\tau_s < \nu + 2$.

We now show that $\tau_s > \mu + 1$. Suppose $\tau_s < \mu + 1$. Then, from Eq. (70), $\mathcal{M}_{\mu+n} \sim M\mathcal{M}_\mu$ and $\mathcal{M}_{\nu+n} \sim$

$M\mathcal{M}_\nu$ for $n \geq 0$. In this case Eq. (68b) simplifies to $\lambda M^2 \mathcal{M}_\mu \mathcal{M}_\nu \sim M^2 \mathcal{M}_\mu \mathcal{M}_\nu$ or $\lambda \sim O(1)$. But λ is a parameter which tends to 0, hence we arrive at a contradiction. Hence, $\tau_s \geq \mu + 1$. We now show that $\tau_s \neq \mu + 1$. In this case, from Eq. (70), it follows that $\mathcal{M}_\mu \sim M^{-\eta_s} \ln M$, $\mathcal{M}_{\mu+n} \sim M\mathcal{M}_\mu / \ln M$, and $\mathcal{M}_{\nu+n} \sim M\mathcal{M}_\nu$ for $n \geq 0$. It is straightforward to show that substituting into Eq. (68a) gives $\lambda \sim M^{-1}$, while substituting into Eq. (68b) gives $\lambda \sim 1/\ln M$, leading to a contradiction. We thus obtain $\tau_s > \mu + 1$. Combining the two bounds:

$$\mu + 1 < \tau_s < \nu + 2. \tag{71}$$

The equations for moments [see Eq. (68)] may be further simplified if only the order of magnitude of the different terms is considered. Consider Eq. (68a). We will argue that the left hand side of Eq. (68a) is dominated by the second term. Let $r = \mathcal{M}_\mu \mathcal{M}_{\nu+1}/(\mathcal{M}_{\mu+1}\mathcal{M}_\nu)$. If the integral Eq. (69) determining $\mathcal{M}_\nu$ does not diverge, then neither will the integral for $\mathcal{M}_\mu$ diverge, implying that $\mathcal{M}_\nu \sim \mathcal{M}_\mu$. Then, $r \sim \mathcal{M}_{\nu+1}/\mathcal{M}_{\mu+1}$. Since $\nu \geq \mu$, clearly $r \sim O(M^x)$ where $x \geq 0$. On the other hand, if the integral for $\mathcal{M}_\nu$ diverges, then $\mathcal{M}_{\nu+1} \sim M\mathcal{M}_\nu$. Then $r \sim \mathcal{M}_\mu M/\mathcal{M}_{\mu+1}$. Since $\mathcal{M}_{\mu+1}/\mathcal{M}_\mu$ can diverge utmost as M, we again obtain $r \sim O(M^x)$ where $x \geq 0$. Equation (68a) then reduces to $\lambda \mathcal{M}_{\nu+1} \sim \mathcal{M}_\nu$, or equivalently $\lambda \sim \mathcal{M}_\nu / \mathcal{M}_{\nu+1}$.

The same reasoning may be used to argue that the left hand side of Eq. (68b) is dominated by the second term. The left hand side is then $\lambda \mathcal{M}_\mu \mathcal{M}_{\nu+2} \sim \mathcal{M}_\mu \mathcal{M}_\nu \mathcal{M}_{\nu+2}/\mathcal{M}_{\nu+1}$, where we substituted for λ. Since $\tau_s < \nu + 2$ [see Eq. (71)], $\mathcal{M}_{\nu+2}/\mathcal{M}_{\nu+1} \sim M$, and the left hand side simplifies to $M\mathcal{M}_\mu \mathcal{M}_\nu$. The right hand side of Eq. (68b) has to be then dominated by $2\mathcal{M}_{\mu+1}\mathcal{M}_{\nu+1}$. The equations for moments [see Eq. (68)] may then be rewritten as

$$\frac{\mathcal{M}_\nu}{\mathcal{M}_{\nu+1}} \sim \lambda, \tag{72a}$$

$$\mathcal{M}_1 \sim 1, \tag{72b}$$

$$\mathcal{M}_{\mu+1}\mathcal{M}_{\nu+1} \sim M\mathcal{M}_\mu \mathcal{M}_\nu, \tag{72c}$$

where Eq. (72b) follows from conservation of mass.

We can now derive τ_s, η_s and y in terms of the known parameters. We have already shown that $\mu + 1 \leq \tau_s < \nu + 2$ [see Eq. (71)]. For this range of τ_s, and applying Eq. (70), we obtain

$$\mathcal{M}_\mu \sim M^{-\eta_s}, \tag{73a}$$

$$\mathcal{M}_{\mu+1} \sim M^{-\eta_s + \max(\mu+2-\tau_s,0)}, \tag{73b}$$

$$\mathcal{M}_\nu \sim M^{-\eta_s + \max(\nu+1-\tau_s,0)}, \tag{73c}$$

$$\mathcal{M}_{\nu+1} \sim M^{-\eta_s + \nu + 2 - \tau_s}. \tag{73d}$$

Substituting Eq. (73) into Eq. (72), we obtain

$$\frac{1}{y} = \nu + 2 - \tau_s - \max(\nu + 1 - \tau_s, 0), \tag{74a}$$

$$\eta_s = \max(2 - \tau_s, 0), \tag{74b}$$

$$\max(\nu + 1 - \tau_s, 0) = \max(\mu + 2 - \tau_s, 0) + \nu + 1 - \tau_s. \tag{74c}$$

To make further progress, we consider different regimes of τ_s. Consider first $\tau_s < \nu + 1$. Equation (74) implies that

$$y = 1, \tag{75a}$$

$$\eta_s = \max(2 - \tau_s, 0), \quad \theta > 1, \tag{75b}$$

$$\mu + 2 \leq \tau_s < \nu + 1, \tag{75c}$$

where we obtained the constraint on θ from requiring that a non-zero interval should exist for the inequality satisfied by τ_s in Eq. (75c). Note that the values of τ_s and η_s cannot be determined using moment analysis alone.

Consider now the second case: $\tau_s > \nu + 1$. In this regime, Equation (74a) implies that $y^{-1} = \nu + 2 - \tau_s$, while Eq. (74c) reduces to

$$\nu + 1 - \tau_s + \max(\mu + 2 - \tau_s, 0) = 0. \tag{76}$$

If $\tau_s \geq \mu + 2$, then Eq. (76) implies that $\tau_s = \nu + 1$ but we had assumed that $\tau_s > \nu + 1$. Therefore, we conclude that $\tau_s < \mu + 2$. This, in conjunction with the assumption $\tau_s > \nu + 1$, implies that $\theta = \nu - \mu < 1$, i.e., the kernel is local. We immediately obtain from Eq. (76) that $\tau_s = (3 + \beta)/2$. Knowing τ_s allows to derive all the exponents. To summarize,

$$\tau_s = \frac{3 + \beta}{2}, \tag{77a}$$

$$\eta_s = \max\left[\frac{1 - \beta}{2}, 0\right], \quad \theta < 1, \tag{77b}$$

$$y = \frac{2}{\theta + 1}. \tag{77c}$$

We now verify numerically that the correctness of Eq. (77a) for $\theta < 1$. In Fig. 4, we show the variation of $N(m)$ with m for two different values of β, and varying $\theta < 1$. The data for $N(m)$ for small masses are independent of θ, and are consistent with a power law with exponent given by Eq. (77a).

Thus when the kernel is local, all exponents describing the small mass behavior of the mass distribution can be obtained using moment analysis, unlike the case when the kernel is non-local. However the analysis of singularities will enable us to determine the unknown exponents.

We now study the case when $\theta = \nu - \mu = 1$, the boundary between the kernel being local or non-local. For this special case, we expect that the power laws will be modified by additional logarithmic corrections [32]. We assume the following form for $N(m)$:

$$N(m) \sim \frac{(\ln m)^{-x}(\ln M)^{-z}}{m^{\nu+1}M^{\eta_s}}, \quad m \ll M, \; \theta = 1, \tag{78}$$
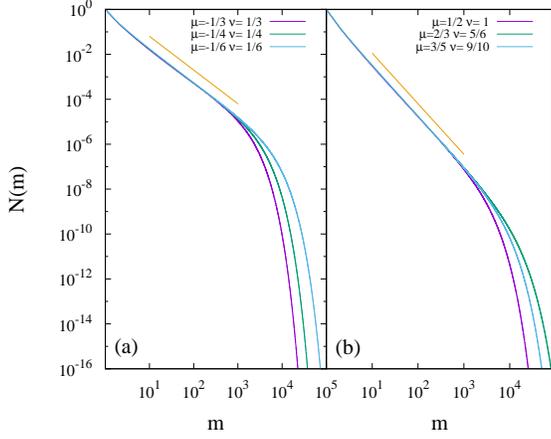
FIG. 4. The steady mass distribution $N(m)$ for kernels with fixed β and different $\theta < 1$. (a) $\beta = 0$ for $\theta = 2/3, 1/2, 1/3$, and (b) $\beta = 3/2$ for $\theta = 1/2, 1/6, 3/10$. The solid lines are power laws with exponents $(3+\beta)/2$, as derived in Eq. (77a). The data are for $\lambda = 0.01$

where the cutoff mass scale M could have a logarithmic dependence on λ, and x and z are new exponents that characterize the logarithmic corrections. The choice of $\tau_s = \nu + 1$ is motivated from $\theta \to 1$ behavior of Eq. (77a). It is then straightforward to obtain $\mathcal{M}_\mu \sim M^{-\eta_s}(\ln M)^{-z}$, $\mathcal{M}_{\mu+1} \sim \mathcal{M}_\nu \sim M^{-\eta_s}(\ln M)^{-z+\max(0,1-x)}$, and $\mathcal{M}_{\nu+1} \sim M^{1-\eta_s}(\ln M)^{-x-z}$. For $\nu = \mu + 1$, Eq. (72c) reduces to $\mathcal{M}_{\nu+1} \sim M\mathcal{M}_\mu$. Substituting for the moments, we immediately obtain

$$x = 0. \tag{79}$$

For this choice of x, Eq. (72a) immediately yields $\lambda \sim M^{-1}\ln M$ or

$$M \sim \frac{-\ln\lambda}{\lambda}, \quad \theta = 1. \tag{80}$$

Substituting for the different moments into Eq. (72b), it is straightforward to derive

$$\eta = \max(1 - \nu, 0), \quad \theta = 1 \tag{81}$$
$$z = \delta_{\nu,1}, \quad \theta = 1. \tag{82}$$

VII. SINGULARITY ANALYSIS

In this section, we analyze the equation [see Eq. (9)] satisfied by the generating functions $F_\mu(x)$ and $F_\nu(x)$, based on their singular behavior. This will allow us to determine the exponents τ_ℓ and η_ℓ [see Eq. (13) for definition]. This in turn, will allow us to determine the exponents τ_s and η_s characterizing the small mass behavior of $N(m)$ for non-local kernels.

Let the singularity of $F_\mu(x)$ closest to the origin be denoted by x_c. Comparing with Eq. (13), we immediately

obtain

$$M = \frac{1}{\ln x_c}. \tag{83}$$

Consider $x = x_c - \epsilon$, $\epsilon \to 0$. If the large behavior of $N(m)$ is as in Eq. (13), then the leading singular behavior of the generating functions F_ν and F_μ close to the singular point is proportional to $\epsilon^{\tau-\nu-1}$ and $\epsilon^{\tau-\mu-1}$ respectively. Depending on the value of τ, $F_\nu(x_c)$ or $F_\mu(x_c)$ may diverge or tend to a constant as $\epsilon \to 0$.

Expressing $F_\nu(x)$ in terms of $F_\mu(x)$ from Eq. (9), we obtain

$$F_\nu(x) = \frac{(1+\lambda)\mathcal{M}_\nu F_\mu(x) - x(1+2\lambda)\mathcal{M}_\mu\mathcal{M}_\nu}{F_\mu(x) - (1+\lambda)\mathcal{M}_\mu}. \tag{84}$$

We now claim that $F_\mu(x_c) = (1+\lambda)\mathcal{M}_\mu$. Suppose this were not the case and $F_\mu(x_c) \neq (1+\lambda)\mathcal{M}_\mu$. Then, the denominator in Eq. (84) may be set to a constant when expanding about x_c, and it follows that $F_\nu(x)$ has the same singular behavior as $F_\mu(x)$ near $x = x_c$. This implies that $\mu = \nu$. When $\mu = \nu$, we have determined the generating function $F_\mu(x)$ exactly (see Sec. IV), and it is easily seen from Eq. (20) that $F_\mu(x_c) = (1+\lambda)\mathcal{M}_\mu$. This contradicts our initial assumption that $F_\mu(x_c) \neq (1+\lambda)\mathcal{M}_\mu$. When $\mu \neq \nu$, $F_\mu(x)$ and $F_\nu(x)$ should have different singular singular behavior near $x = x_c$, again leading to a contradiction. We therefore conclude that

$$F_\mu(x_c) = (1+\lambda)\mathcal{M}_\mu. \tag{85}$$

Expanding the generating functions about $x = x_c$, we obtain

$$F_\mu(x_c - \epsilon) = (1+\lambda)\mathcal{M}_\mu - \epsilon^{\tau_\ell - \mu - 1}R_1(\epsilon) - \epsilon R_2(\epsilon), \tag{86a}$$

$$F_\nu(x_c - \epsilon) = \epsilon^{\tau_\ell - \nu - 1}R_3(\epsilon) + R_4(\epsilon), \tag{86b}$$

where R_i's are regular in ϵ, $R_1(0) \neq 0$, and $R_3(0) \neq 0$. Also,

$$\tau_\ell > \mu + 1, \tag{87}$$

so that Eq. (85) is satisfied. We now examine the numerator of Eq. (84) when $x = x_c$. On simplifying by using Eq. (85), it reduces to $(1+2\lambda)\mathcal{M}_\mu\mathcal{M}_\nu[1+\lambda^2-x_c+O(\lambda^3)]$. However, $x_c \sim 1 + M^{-1} \sim 1 + \lambda^y$ when $\lambda \to 0$. We have shown earlier that $y < 2$ for $\theta > 0$ [see Eq. (75a) and Eq. (77c)]. Thus, the numerator of Eq. (84) is nonzero and equal to $-\mathcal{M}_\mu\mathcal{M}_\nu M^{-1}$, when $x = x_c$, $\lambda \to 0$, and $\theta > 0$. Substituting the expansions [Eq. (86)] into Eq. (84) we obtain

$$\epsilon^{\tau_\ell - \nu - 1}R_3(\epsilon) + R_4(\epsilon) = \frac{-\mathcal{M}_\mu\mathcal{M}_\nu M^{-1}}{-\epsilon^{\tau_\ell - \mu - 1}R_1(\epsilon) + \epsilon R_2(\epsilon)}. \tag{88}$$

Since $\tau_\ell > \mu + 1$ [see Eq. (87)], the right hand side of Eq. (88) diverges. This implies that

$$\tau_\ell < \nu + 1, \tag{89}$$

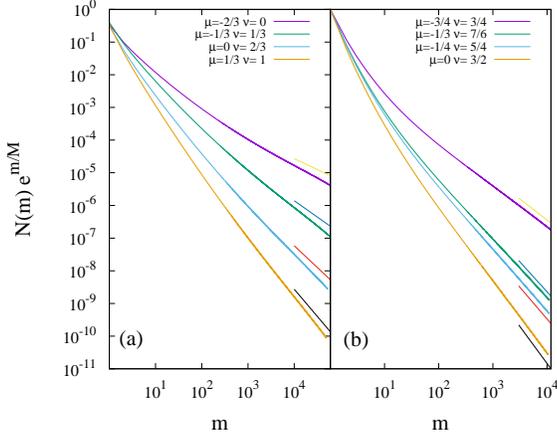and the left hand side of Eq. (88) is dominated by the first term. We can now compare the leading singular behavior on both sides of Eq. (88). There are two possible cases: $0 < \tau_\ell - \mu - 1 < 1$ and $0 < \tau_\ell - \mu - 1 > 1$.

FIG. 5. The compensated steady mass distribution $N(m)e^{m/M}$ for kernels with fixed $\theta < 2$ and different β. (a) $\theta = 2/3$ for $\beta = -2/3, 0, 2/3, 4/3$ and (b) $\theta = 3/2$ for $\beta = 0, 5/6, 1, 3/2$. The solid lines are power laws with exponents $(2+\beta)/2$, as derived in Eq. (90). The data are for $\lambda = 0.01$.

A. $\tau_\ell - \mu - 1 < 1$

First consider the regime $0 < \tau_\ell - \mu - 1 < 1$. The denominator of Eq. (88) is dominated by $-\epsilon^{\tau_\ell - \mu - 1} R_1(\epsilon)$, and comparing the singular terms on both sides, we obtain

$$\tau_\ell = \frac{\beta + 2}{2}, \quad \theta < 2, \tag{90}$$

where we obtain the constraint on θ from our assumption $0 < \tau_\ell - \mu - 1 < 1$. We now verify numerically that the correctness of Eq. (90) for $\theta < 2$. In Fig. 5, we show the variation of $N(m)$ with m for two values of θ, one between zero and one and the other between one and two, and varying β. The data for compensated mass distribution for large masses are consistent with a power law with exponent given by Eq. (90).

Comparing now the coefficients of the leading singular terms we obtain

$$R_3(0)R_1(0) = \mathcal{M}_\mu \mathcal{M}_\nu M^{-1}, \quad \theta < 2. \tag{91}$$

Once $R_1(0)$, $R_3(0)$ and τ_ℓ are known, $m^\mu N(m)$ and $m^\nu N(m)$ may be obtained from $F_\mu(x)$ and $F_\nu(x)$ by doing inverse Laplace transforms. Thus

$$m^\mu N(m) = \frac{-R_1(0)x_c^{\tau_\ell - \mu - 1}(\tau_\ell - \mu - 1)}{x_c^m m^{\tau_\ell - \mu} \Gamma(2 - \tau_\ell + \mu)}, \tag{92}$$

$$m^\nu N(m) = \frac{R_3(0)x_c^{\tau_\ell - \nu - 1}(\tau_\ell - \nu - 1)}{x_c^m m^{\tau_\ell - \nu} \Gamma(2 - \tau_\ell + \nu)}. \tag{93}$$

where $\Gamma(x)$ is the Gamma function. Multiplying together Eqs. (92), and (93), setting $\tau_\ell = (2 + \beta)/2$ [see Eq. (90)], and using the property

$$\Gamma(x)\Gamma(1 - x) = \frac{\pi}{\sin(\pi x)}, \tag{94}$$

we obtain

$$N(m) \simeq \sqrt{\frac{\mathcal{M}_\mu \mathcal{M}_\nu \theta \sin \frac{\pi\theta}{2}}{2\pi M}} \frac{e^{-m/M}}{m^{(2+\beta)/2}}, \quad m \gg M, \tag{95}$$

for $0 < \theta < 2$. The prefactor depends on $\mathcal{M}_\mu$ and $\mathcal{M}_\nu$, which are determined by the behavior of $N(m)$ at small masses. Their dependence on the cutoff M [see Eq. (73)] will determine η_ℓ:

$$\eta_\ell = \frac{1}{2} + \eta_s - \frac{1}{2}\max(\nu + 1 - \tau_s, 0). \tag{96}$$

Knowing $\tau_\ell = (2 + \beta)/2$ [see Eq. (90)], the relation $\tau_s + \eta_s = \tau_\ell + \eta_\ell$ [see Eq. (14)] reduces to

$$\tau_s = \frac{3 + \beta}{2} - \frac{1}{2}\max(\nu + 1 - \tau_s, 0). \tag{97}$$

We consider the two cases $\nu + 1 - \tau_s < 0$ and $\nu + 1 - \tau_s > 0$ separately.

Case I: $\nu + 1 - \tau_s < 0$: In this case Eq. (97) immediately gives $\tau_s = (3 + \beta)/2$. To satisfy the inequality $\nu + 1 - \tau_s < 0$, we require that $\theta < 1$. This result for τ_s is consistent with what we derived earlier for the local kernel using moment analysis [see Eq. (77a)]. Knowing τ_s and $\eta_s = \max[(1 - \beta)/2, 0]$ [see Eq. (77b)], we obtain from Eq. (96)

$$\eta_\ell = \frac{1}{2} + \max\left[\frac{1 - \beta}{2}, 0\right], \quad \theta < 1. \tag{98}$$

Case II: $\nu + 1 - \tau_s > 0$: In this case Eq. (97) immediately gives

$$\tau_s = 2 + \mu = \frac{4 + \beta - \theta}{2}, \quad 1 < \theta < 2, \tag{99}$$

where the constraint on θ is obtained from the inequality $\nu + 1 - \tau_s < 0$. This result for τ_s is consistent with the inequality derived for τ_s using moment analysis [see Eq. (75c)], Knowing τ_s, η_s and η_ℓ may be derived from the Eq. (75b) and Eq. (96) to be

$$\eta_s = \max[-\mu, 0], \quad 1 < \theta < 2, \tag{100}$$

$$\eta_\ell = \frac{2 - \theta}{2} + \max[-\mu, 0], \quad 1 < \theta < 2. \tag{101}$$

For $\tau_s = \mu + 2$, then there is the possibility of logarithmic corrections.

Thus, we have derived all the exponents characterizing both the small and large mass behavior of $N(m)$ when $\theta < 2$.

B. $\tau_\ell - \mu - 1 > 1$

Consider now the second case when $\tau_\ell - \mu - 1 > 1$. The denominator of Eq. (88) is dominated by $\epsilon R_2(\epsilon)$. Again comparing the singular terms on both sides of Eq. (88), we obtain

$$\tau_\ell = \nu, \quad \theta > 2, \tag{102}$$

where we obtain the constraint in θ from our assumption $\tau_\ell - \mu - 1 > 1$. Comparing the coefficients of the leading singular terms we obtain

$$R_2(0)R_3(0) = \mathcal{M}_\mu \mathcal{M}_\nu M^{-1}, \quad \theta > 2. \quad (103)$$

It is easy to see that $R_2(0) = F_{\mu+1}(x_c)$. Doing an inverse Laplace transform, we obtain

$$N(m) \simeq \frac{m^{-\nu}}{M F_{\mu+1}(x_c)} e^{-m/M}, \; m \gg M, \; \theta > 2. \quad (104)$$

The dependence of $R_2(0) = F_{\mu+1}(x_c)$ on M may be determined as follows. The integral for $F_{\mu+1}(x_c)$ has two power laws:

$$F_{\mu+1}(x_c) \sim \int^M dm \frac{m^{\mu+1}}{M^{\eta_s} m^{\tau_s}} + \int_M^\infty dm \frac{m^{\mu+1}}{M^{\eta_\ell} m^\nu} \quad (105)$$

Using the bound Eq. (75c), it is straightforward to argue that to leading order $F_{\mu+1}(x_c) \sim M^{-\min(\eta_s, \eta_\ell + \theta - 2)}$. Substituting $R_3(0) \sim M^{-\eta_\ell}$ and $R_2(0) \sim M^{-\min(\eta_s, \eta_\ell + \theta - 2)}$ into Eq. (103), we immediately obtain

$$\eta_\ell + \min(\eta_s, \eta_\ell + \theta - 2) = 2\eta_s, \quad \theta > 2. \quad (106)$$

We consider the two cases $\eta_s < \eta_\ell + \theta - 2$ and $\eta_s > \eta_\ell + \theta - 2$ separately.

Case I: $\eta_s < \eta_\ell + \theta - 2$: From Eq. (106), we obtain

$$\eta_\ell = \eta_s, \quad \theta > 2, \quad (107)$$

where the constraint on θ is obtained from the assumption that $\eta_s < \eta_\ell + \theta - 2$. Equation (14) then yields $\tau_s = \tau_\ell$. Therefore, Eq. (102) and Eq. (75b) imply that

$$\tau_s = \nu, \quad (108)$$
$$\eta_s = \max(2 - \nu, 0), \quad \theta > 2, \quad (109)$$
$$\eta_\ell = \max(2 - \nu, 0). \quad (110)$$

Case II: $\eta_s > \eta_\ell + \theta - 2$: From Eq. (106), we obtain

$$\eta_\ell = \eta_s + 1 - \frac{\theta}{2}. \quad (111)$$

This solution in conjunction with our assumption that $\eta_s > \eta_\ell + \theta - 2$ imply that $\theta < 2$. But, the solution Eq. (102) is valid only for $\nu > 2$. Hence there is no solution for this case. We note that the results for τ_ℓ and η_ℓ coincide with those for the addition model when $\theta > 2$ [see Eq. (30)] .

We now verify numerically that the correctness of Eq. (108) for $\theta > 2$. In Fig. 6, we show the variation of $N(m)$ with m for two values of ν, for different values of $\theta > 2$. The data for compensated mass distribution for large masses are consistent with a power law with exponent given by Eq. (108).
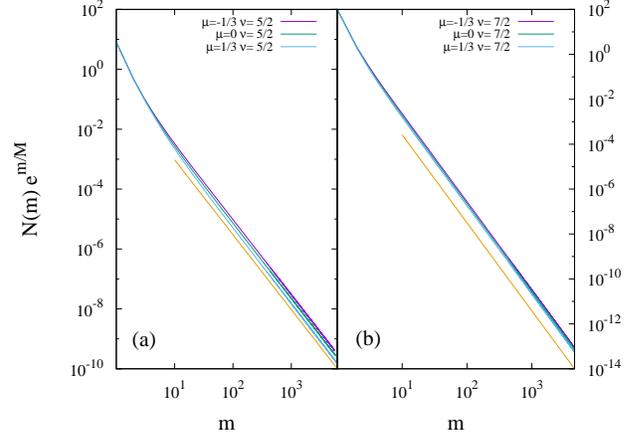

FIG. 6. L $\nu = 1.5; \mu = -1$. R $\nu = 2.5; \mu = -0.33$. L Does not scale as λ^{η_S} The compensated steady mass distribution $N(m)e^{m/M}$ for kernels with fixed ν and different $\theta > 2$. (a) $\nu = 5/2/$ for $\theta = 17/6, 5/2, 13/6$ and (b) $\nu = 7/2/$ for $\theta = 23/6, 7/2, 19/6$. The solid lines are power laws with exponents ν, as derived in Eq. (108). The data are for $\lambda = 0.01$.

VIII. CONCLUSION

In this paper, we determined the steady state mass distribution for a system of particles that on undergoing two-body collisions either coalesce into a single particle or fragment into dust (particles of the smallest mass). The total mass is conserved by the dynamics. Fragmentation acts as a source of particles of small mass while coagulation depletes smaller particles and creates particles of larger mass. We considered a class of homogeneous collision kernels modeled by $K(m_1, m_2) = m_1^\mu m_2^\nu + m_1^\nu m_2^\mu$ with $\nu \geq \mu$, characterized by the homogeneity exponent $\beta = \mu + \nu$ and non-locality exponent $\theta = \nu - \mu$. The results for the exponents characterizing the small and large mass distributions, obtained through a combination of moment analysis, singularity analysis, and exact solutions for special cases, are summarized in Table I for different β and θ.

The presence of a non-zero fragmentation rate λ introduces a cutoff scale M beyond which the mass distribution $N(m)$ crosses over from a power law behavior to an exponential decay with increasing mass m. Thus, a non-zero λ is a useful regularisation scheme by which instantaneous gelation is prevented for kernels that are gelling ($\mu + \nu > 1$) and one may study the behavior as the regularisation is removed by taking the limit $\lambda \to 0$. Here, we find that the form of $N(m)$ depends only on whether the kernel is local ($\theta < 1$) or non-local ($\theta \geq 1$) and not on whether it is gelling or non-gelling.

We find two distinct non-local regimes corresponding to $1 < \theta < 2$ and $\theta > 2$. When $\theta < 1$, the distribution is universal in the sense that the small mass behavior does not depend on the source or sink. Thus, the limit $\lambda \to 0$ is well defined. In the regime, $1 < \theta < 2$ the
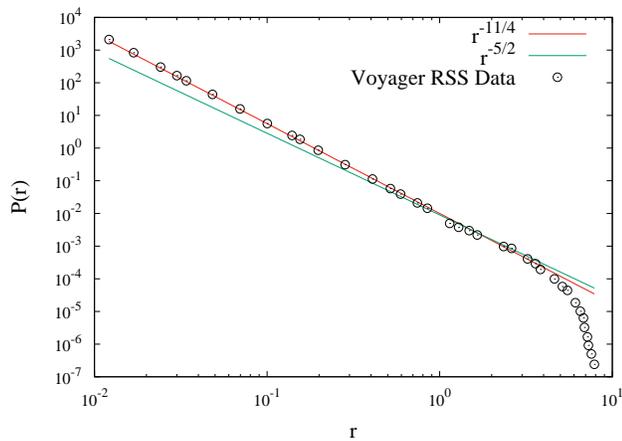
FIG. 7. The data (extracted from Ref. [25]) for the particle size distribution of Saturn's A ring measured by the Voyager Radio Science Subsystem [42] are compared with power laws (solid lines) $r^{-11/4}$ and $r^{-5/2}$.

mass distribution $N(m)$ depends on the sink scale M but is independent of the source scale, m_0. In the regime $\theta > 2$, $N(m)$ depends on both source and sink. Logarithmic corrections are found at the boundaries between regimes. These are similar to the two non-local regimes that we found for the non-conserved model driven by input of particles at small masses and collision dependent evaporation [32]. The logarithmic corrections are also analogous to the correction proposed by Kraichnan [41] to account for the marginal non-locality of the enstrophy cascade in two-dimensional fluid turbulence.

The model studied in this paper was introduced as a model for describing the dynamics of the clusters of ice and dust that constitute the rings of Saturn [25]. The relevant collision kernel is the one valid for ballistic motions: $K(m_1, m_2) = |m_1^{-1/2} - m_2^{-1/2}|(m_1^{1/3} + m_2^{1/3})^2$, corresponding to $\nu = 2/3$, $\mu = -1/2$ or equivalently $\beta = 1/6$ and $\theta = 7/6$. Due to this kernel being not solvable, the mass distribution was worked out for the kernel $K(m_1, m_2) = (m_1 m_2)^{1/12}$ which has the same value of β, but with $\theta = 0$, instead of $\theta = 7/6$. These results were compared with the experimental data on the mass distribution of rings of Saturn, and an excellent agreement was found [25]. However, the ballistic kernel is nonlocal ($\theta > 1$), and from the analysis in the current study, the results are different from $\theta = 0$, even though β is the same. In Fig. 7, we compare the data (extracted from Ref. [25]) for the radius distribution ($P(r)$) of Saturn's A ring measured by the Voyager Radio Science Subsys-

tem [42] with the analytical solutions $r^{-11/4}$ as obtained in Ref. [25] and $r^{-5/2}$ as obtained in this paper. While both the distributions describe the large mass data well, the distribution $r^{-11/4}$ describe the data at small masses also.

We find that the results for $\theta > 2$ coincide with that for addition model in which clusters grow in size only when they react with a monomer. The time dependent as well as steady state solutions have been determined for this simpler model [33–38]. However its applicability for more general kernels has not clearly been spelt out. Here, we delineate clearly its role for more general kernels by showing that the addition model is a good description of systems with $\theta > 2$.

In this paper, we studied the steady state but not the dynamics leading to it. This question is important to consider. Even in the local case, $\theta < 1$, the dynamics leading to the steady state must be very different for gelling ($\beta > 1$) and non-gelling ($\beta < 1$) kernels. Furthermore, in the non-local case, evidence from closely related models [36, 43] suggests that the steady state could become unstable for $\lambda \to 0$. Such an instability would result in persistent oscillatory kinetics. Indeed, such oscillations have been seen in a recent paper [44]. This would have interesting prediction for the mass distribution in Saturn rings which could be experimentally verifiable.

In other models of aggregation and fragmentation, where fragmentation occurs spontaneously and not due to a collision, an interesting phase transition occurs when the fragmentation is limited to a finite mass chipping off to a neighbor [45–50]. This model undergoes a nonequilibrium phase transition from a phase in characterized by an exponential mass distribution to a phase characterized by power law mass distribution in the presence of a condensate. The condensate is one single mass which carries a finite fraction of the total mass. It would be interesting to see whether the model considered in the paper exhibits a similar transition in some parameter regimes.

In this paper, we have assumed that the system is well mixed, and hence it was possible to ignore spatial variations in the densities. Also, the effects of stochasticity were completely ignored. Introducing stochasticity, even at the level of zero dimensions, can give rise to new phenomenology like an absorbing-active phase transition in the λ-density plane. This is because, if total mass is small enough, then the system has a finite probability of getting stuck in an absorbing state where all particles have coalesced into one particle. Including spatial variation would make the problem even richer. This is a promising area for future study.

[1] J. Berger, M. Reist, J. Mayer, O. Felt, and R. Gurny, Euro. J. Pharma. Biopharma. **57**, 35 (2004).

[2] N. M. Sangeetha and U. Maitra, Chem. Soc. Rev. **34**, 821 (2005).

[3] S. Friedlander, *Smoke, Dust, and Haze: Fundamentals of Aerosol Dynamics*, Topics in chemical engineering (Oxford University Press, 2000).

[4] G. Falkovich, A. Fouxon, and M. G. Stepanov, Nature

419, 151 (2002).

[5] P. Horvai, S. V. Nazarenko, and T. H. M. Stein, J. Stat. Phys. **130**, 1177 (2008).

[6] A. Pineau, A. A. Benzerga, and T. Pardoen, Acta Mater. **107**, 424 (2016).

[7] A. M. Tom, R. Rajesh, and S. Vemparala, J. Chem. Phys. **144**, 034904 (2016).

[8] A. M. Tom, R. Rajesh, and S. Vemparala, arXiv preprint arXiv:1706.10109 (2017).

[9] F. Leyvraz, Phys. Rep. **383**, 95 (2003).

[10] C. Connaughton, R. Rajesh, and O. Zaboronski, in *Handbook of Nanophysics: Clusters and Fullerenes*, edited by K. D. Sattler (Taylor and Francis, 2010).

[11] K. Wada, H. Tanaka, T. Suyama, H. Kimura, and T. Yamamoto, Astrophys. J. **702**, 1490 (2009).

[12] N. V. Brilliantov, A. S. Bodrova, and P. L. Krapivsky, J. Stat. Mech. **2009**, P06011 (2009).

[13] A. Nakamura and A. Fujiwara, Icarus **92**, 132 (1991).

[14] I. Giblin, G. Martelli, P. Farinella, P. Paolicchi, M. Di Martino, and P. Smith, Icarus **134**, 77 (1998).

[15] M. Arakawa, Icarus **142**, 34 (1999).

[16] F. Kun, F. Wittel, H. Herrmann, B. Kröplin, and K. Måløy, Phys. Rev. Lett. **96**, 025504 (2006).

[17] F. Spahn, E. V. Neto, A. H. F. Guimarães, A. N. Gorban, and N. V. Brilliantov, New J. Phys. **16**, 013031 (2014).

[18] D. Dhar, J. Phys. A **48**, 175001 (2015).

[19] D. Grady and J. Lipkin, Geophys. Res. Lett. **7**, 255 (1980).

[20] P. Michel, W. Benz, and D. C. Richardson, Nature **421**, 608 (2003).

[21] A. Nakamura, T. Michikami, N. Hirata, A. Fujiwara, R. Nakamura, M. Ishiguro, H. Miyamoto, H. Demura, K. Hiraoka, T. Honda, C. Honda, J. Saito, T. Hashimoto, and T. Kubota, Earth Planets Space **60**, 7 (2008).

[22] J. A. Åström, D. Vallot, M. Schäfer, E. Z. Welty, S. O'neel, T. Bartholomaus, Y. Liu, T. Riikilä, T. Zwinger, J. Timonen, and J. C. Moore, Nat. Geosci. **7**, 874 (2014).

[23] D. R. Davis, S. J. Weidenschilling, C. R. Chapman, and R. Greenberg, Science **224**, 744 (1984).

[24] P.-Y. Longaretti, Icarus **81**, 51 (1989).

[25] N. Brilliantov, P. Krapivsky, A. Bodrova, F. Spahn, H. Hayakawa, V. Stadnichuk, and J. Schmidt, Proc. Nat. Acad. Sci. **112**, 9536 (2015).

[26] J. N. Cuzzi *et al.*, Science **327**, 1470 (2010).

[27] J. C. Bohorquez, S. Gourley, A. R. Dixon, M. Spagat, and N. F. Johnson, Nature **462**, 911 (2009).

[28] N. F. Johnson, J. Ashkenazi, Z. Zhao, and L. Quiroga, AIP Advances **1**, 012114 (2011).

[29] B. K. Teh and S. A. Cheong, PloS one **11**, e0163842 (2016).

[30] C. Connaughton, R. Rajesh, and O. Zaboronski, Phys. Rev. E **69**, 061114 (2004).

[31] M. V. Smoluchowski, Z. Phys. Chem. **92**, 129 (1917).

[32] C. Connaughton, A. Dutta, R. Rajesh, and O. Zaboronski, Euro. Phys. Lett. **117**, 10002 (2017).

[33] E. Hendriks and M. Ernst, J. Coll. Inter. Sci. **97**, 176 (1984).

[34] N. V. Brilliantov and P. L. Krapivsky, J. Phys. A **24**, 4789 (1991).

[35] P. Laurençot, Nonlinearity **12**, 229 (1999).

[36] R. C. Ball, C. Connaughton, T. H. M. Stein, and O. Zaboronski, Phys. Rev. E **84**, 011111 (2011).

[37] J. Blackman and A. Marshall, J. Phys. A **27**, 725 (1994).

[38] F. Chávez, M. Moreau, and L. Vicente, J. Phys. A **30**, 6615 (1997).

[39] S. Chatterjee, P. Pradhan, and P. Mohanty, Phys. Rev. Lett. **112**, 030601 (2014).

[40] A. Das, S. Chatterjee, and P. Pradhan, Phys. Rev. E **93**, 062135 (2016).

[41] R. H. Kraichnan, J. Fluid. Mech. **47**, 525 (1971).

[42] H. A. Zebker, E. A. Marouf, and G. L. Tyler, Icarus **64**, 531 (1985).

[43] R. C. Ball, C. Connaughton, P. P. Jones, , R. Rajesh, and O. Zaboronski, Phys. Rev. Lett. **109**, 168304 (2012).

[44] S. Matveev, P. Krapivsky, A. Smirnov, E. Tyrtyshnikov, and N. Brilliantov, arXiv preprint arXiv:1708.01604 (2017).

[45] S. N. Majumdar, S. Krishnamurthy, and M. Barma, Phys. Rev. Lett **81**, 3691 (1998).

[46] S. N. Majumdar, S. Krishnamurthy, and M. Barma, J. Stat. Phys. **99**, 1 (2000).

[47] P. Krapivsky and S. Redner, Phys. Rev. E **54**, 3553 (1996).

[48] R. Rajesh and S. Majumdar, Phys. Rev. E **63**, 036114 (2001).

[49] R. Rajesh and S. Krishnamurthy, Phys. Rev. E **66**, 046132 (2002).

[50] R. Rajesh, D. Das, B. Chakraborty, and M. Barma, Phys. Rev. E **66**, 056104 (2002).